Composition dependence of glass transition temperature and fragility. I. A topological model incorporating temperature-dependent constraints

Prabhat K. Gupta and John C. Mauro

Citation: J. Chem. Phys. **130**, 094503 (2009); doi: 10.1063/1.3077168
View online: http://dx.doi.org/10.1063/1.3077168
View Table of Contents: http://jcp.aip.org/resource/1/JCPSA6/v130/i9
Published by the American Institute of Physics.

Composition dependence of glass transition temperature and fragility. I. A topological model incorporating temperature-dependent constraints

Prabhat K. Gupta[1] and John C. Mauro[2,a)]
[1]*Department of Materials Science and Engineering, Ohio State University, Columbus, Ohio 43210, USA*
[2]*Science and Technology Division, Corning Incorporated, SP-TD-01-01, Corning, New York 14831, USA*

(Received 17 November 2008; accepted 12 January 2009; published online 5 March 2009)

We present a topological model for the composition dependence of glass transition temperature and fragility. Whereas previous topological models are derived for zero temperature conditions, our approach incorporates the concept of temperature-dependent constraints that freeze in as the system is cooled from high temperature. Combining this notion of temperature-dependent constraints with the Adam–Gibbs model of viscosity, we derive an analytical expression for the scaling of glass transition temperature and fragility in the binary Ge_xSe_{1-x} system. In the range of $0 \leq x \leq 1/3$, we reproduce the modified Gibbs–DiMarzio equation of Sreeram *et al.* [J. Non-Cryst. Solids **127**, 287 (1991)] but without any empirical fitting parameters. The modified Gibbs–DiMarzio equation breaks down for $1/3 < x \leq 2/5$, where the glass transition temperature decreases with increasing germanium content. © *2009 American Institute of Physics*. [DOI: 10.1063/1.3077168]

I. INTRODUCTION

Every step of industrial glass production—melting, fining, forming, and annealing—is governed by the shear viscosity (η) of the melt.[1,2] From the initial glass melting to a final forming, viscosity varies by over 12 orders of magnitude. Viscosity is also sensitive to small changes in composition, especially in silicate melts where small levels of impurities can have a profound influence on the flow behavior. It is thus of great importance to have accurate knowledge of the scaling of viscosity with both composition (x) and temperature (T). Unfortunately, measurement of $\eta(T,x)$ is challenging for high temperature melts, and low temperature measurements (i.e., in the high viscosity range, 10^{10}–10^{15} Pa s) are time consuming[1,3,4] and often prohibitively expensive. It is therefore of great interest to develop an accurate model of $\eta(T,x)$.

Modeling of viscosity has been attempted at several levels. On one extreme are empirical models, such as the highly successful Vogel–Fulcher–Tamman (VFT) model,[1,5,6]

$$\log_{10}\ \eta(T,x) = A(x) + \frac{B(x)}{T - T_{\mathrm{VFT}}(x)}. \tag{1}$$

The three VFT parameters (A, B, and T_{VFT}) are obtained by fitting Eq. (1) to the experimentally measured viscosity data. On the other extreme are atomistic models, which generally employ the Green–Kubo formalism and always assume an accurate knowledge of the interatomic potentials. However, calculations for real systems require large computational times and have been attempted only for a limited number of simple fluids.[7,8] Furthermore, the small integration time step required in molecular dynamics prohibits these simulations from accessing the long time scales necessary to compute high values of viscosity.[9]

Most successful models of viscosity are intermediate level (macroscopic) models that not only relate viscosity to some fundamental quantity but also contain a small set of empirical fitting parameters. An example is the Adam–Gibbs model[10–15] that describes $\eta(T,x)$ in terms of the configurational entropy, $S_c(T,x)$, of the melt,

$$\log_{10}\ \eta(T,x) = A(x) + \frac{B(x)}{TS_c(T,x)}. \tag{2}$$

The fitting parameters A and B are independent of temperature but may be dependent on composition. Use of the Adam–Gibbs equation requires a knowledge of $S_c(T,x)$, which is usually obtained by integrating experimental heat capacity curves.

While it is desirable to model the entire $\eta(T,x)$ surface, there are really two parameters of particular importance: the glass transition temperature (T_g) and the fragility (m) of the melt. Both can be obtained from knowledge of $\eta(T,x)$. The glass transition temperature represents the upper use temperature limit of a glass and also the low temperature limit for glass-forming operations. For any composition, the glass transition temperature is defined as the temperature at which the shear viscosity is equal to some fixed value, generally taken as 10^{12} Pa s,[1,3]

$$\eta(T_g(x),x) = 10^{12}\ \text{Pa s}. \tag{3}$$

The (kinetic) fragility m describes the rate at which the viscosity changes with temperature at T_g. Fragility is defined as[16–32]

$$m(x) \equiv \left.\frac{\partial \log_{10}\ \eta}{\partial(T_g/T)}\right|_{T=T_g(x)}. \tag{4}$$

The pioneering work of Phillips and Thorpe[33–38] demonstrated that great insight can be gained into the composition dependence of glass properties by analyzing the topology of

a)Electronic mail: mauroj@corning.com.

the glassy network. The Phillips–Thorpe approach is based on comparing the number of atomic degrees of freedom with the number of interatomic force field constraints.[33] If the number of degrees of freedom is greater than the number of constraints, the network is "floppy;" conversely, if the network becomes overconstrained, stressed-rigid structures will percolate throughout the entire network.[34–38] Phillips[33] conjectured that the tendency for glass formation would be maximized when the number of degrees of freedom exactly equals the number of constraints.

In the Phillips–Thorpe approach, the number of constraints is determined by counting the number of bond lengths and bond angles in the system. A mathematically equivalent approach has been derived by Gupta and Cooper,[39–43] but treating the network in terms of rigid polytopes connected at vertices. With both the Phillips–Thorpe and Gupta–Cooper approaches, the number of constraints for a given composition is constant with respect to temperature. In other words, these models are formulated for zero temperature conditions, where there is no thermal energy to overcome the bond length or angular constraints. Without including temperature effects, it is impossible to calculate $T_g(x)$ and $m(x)$ from either model.

The purpose of this paper is to present a topological model for $T_g(x)$ and $m(x)$ accounting for the *temperature-dependent nature of constraints*. Our model is based on the following postulates.

(1) The spatially-averaged atomic level structure of a glass just below its glass transition temperature is the same as that of the liquid just above the glass transition temperature. This structure can be viewed as an infinitely large topologically disordered network of bond constraints.
(2) The network can be floppy (underconstrained), isostatic (optimally constrained), or stressed rigid (overconstrained) depending on the average number of constraints per atom $n(T,x)$ and the network dimensionality (d). When $n(T,x)<d$, the network is underconstrained and contains low-frequency deformation modes, called floppy modes. The network is optimally rigid when $n(T,x)=d$ and is stressed rigid when $n(T,x)>d$.
(3) For a given composition x at high temperatures, the number of constraints is low and the network is floppy. As the temperature is lowered, more constraints are "frozen in." At some temperature $T_0(x)$ the system becomes optimally rigid, $n[T_0(x),x]=d$, and the viscosity diverges. In terms of Eqs. (1) and (2), $T_0(x)=T_{\mathrm{VFT}}(x)$ and $S_c[T_0(x)]=0$. It is clear that $T_g(x)>T_0(x)$ for all realistic glass-forming systems.
(4) For $T<T_0(x)$, additional constraints become rigid. However, these constraints are redundant and do not affect the global rigidity of the network. (They do, however, act to increase the shear modulus of the glass.)

The outline of our paper is as follows. In Sec. II, we justify the notion of temperature-dependent constraints in terms of the energy landscape approach. We then derive the basic equations for calculating $T_g(x)$ and $m(x)$ in Sec. III. In Sec. IV, we derive a topological model for the binary Ge_xSe_{1-x} system and compare the predicted $T_g(x)$ and $m(x)$ with experimental results.

II. TEMPERATURE-DEPENDENT CONSTRAINTS AND THE ENERGY LANDSCAPE APPROACH

Traditional atomistic simulation techniques such as molecular dynamics involve integrating the equations of motion using a time step on the order of 10^{-15} s. It is thus infeasible to use these techniques to achieve the long time scales involved in the study of supercooled liquid and glassy dynamics.[9] In 1969, Goldstein[44] postulated that atomic motion in a supercooled liquid consists of high-frequency vibrations in deep potential energy minima and less frequent transitions to other such minima. By separating the high-frequency vibrations within minima from the low-frequency transitions between minima, this so-called "energy landscape" approach greatly facilitates study of supercooled liquid and glassy dynamics. For simulations at constant pressure, the landscape formalism can be rewritten in terms of an enthalpy landscape.[45–49]

For a system of N atoms in d dimensions, the potential energy landscape is a dN-dimensional hypersurface containing a multitude of local minima. Each of these minima corresponds to a mechanically stable configuration of atoms known as an "inherent structure."[50–55] The volume of configurational space that drains to a particular minimum via steepest descent is called a "basin;" there is exactly one basin for every inherent structure. While the landscape itself is independent of temperature, the way in which the system explores the landscape in time depends on its phonon energy, and hence on the temperature of the system. At high temperatures, the system can flow freely among basins, corresponding to the case of an equilibrium liquid. As the system is cooled, the interbasin transitions occur less frequently due to the loss of thermal energy. Finally, the glassy state at low temperatures corresponds to a breakdown of ergodicity where the system becomes trapped in a subset of the overall phase space known as a "metabasin."[56]

The energy landscape defines the set of all possible basins, each basin being associated with an inherent structure that defines the configuration and hence the topology of the network. Escape from a given basin involves transitioning through some saddle point and often involves the breaking of a constraint. The ability of a system to overcome this constraint, and hence the rigidity provided by the constraint, is strongly dependent on the temperature of the system. Letting $q(T)$ denote the degree of rigidity of a given constraint, it is thus apparent that

$$\lim_{T\to 0} q(T) = 1 \quad \text{and} \quad \lim_{T\to\infty} q(T) = 0. \tag{5}$$

In the limit of zero temperature there is no thermal energy available to break the constraint, so the constraint is fully rigid. In the limit of infinite temperature, the constraint is easily broken and hence does not contribute to the rigidity of the network. At a finite temperature, some fraction of the constraints are broken while others are rigid. In terms of the

energy landscape approach, $q(T)$ can be expressed as[56]

$$q(T) = \left[1 - \exp\left(-\frac{\Delta F^*}{kT}\right)\right]^{\nu t_{\text{obs}}}, \tag{6}$$

where ΔF^* is the activation free energy for breaking a constraint, k is Boltzmann's constant, ν is the vibrational attempt frequency, and t_{obs} is the observation time. Since typically νt_{obs} is large, $q(T)$ can be approximated by a unit step function,

$$q(T) = \theta(T_q - T), \tag{7}$$

where T_q represents the temperature below which a particular constraint becomes rigid.

III. THE COMPOSITION DEPENDENCE OF GLASS TRANSITION TEMPERATURE AND FRAGILITY

According to the Gibbs–DiMarzio theory of the glass transition,[57] the fluidity of a system depends directly on the configurational entropy. This argument of entropy-dependent flow was subsequently used by Adam and Gibbs[10] to develop an entropy-based theory of structural relaxation that describes the viscosity-temperature relationship of a liquid. The central assumption of the Adam–Gibbs theory is that a liquid consists of a number of independently relaxing regions or subsystems. Each region is composed of a group of atoms or molecules that can rearrange cooperatively. As the liquid is supercooled the configurational entropy of the system diminishes and the size of the cooperatively rearranging subsystems grows progressively larger. With the Adam–Gibbs relation of Eq. (2), the viscosity of a given composition x can be computed as a function of its configurational entropy. Since the extrapolated infinite temperature viscosity is generally independent of composition,[16] $A(x)=\log_{10}\eta_\infty$, and Eq. (2) becomes

$$\log\ \eta_{10}(T,x) = \log_{10}\ \eta_\infty + \frac{B(x)}{TS_c(T,x)}. \tag{8}$$

Although the Adam–Gibbs model provides important insights into the relationship between configurational entropy and the transport coefficients of a supercooled liquid, it fails to provide a means for calculating $B(x)$, which is left as a fitting parameter. In this section, we make use of the Adam–Gibbs model in a topological approach to compute the scaling of glass transition temperature and fragility with composition.

Suppose we wish to compute the glass transition temperature of a certain composition x with respect to some other reference composition x_R. Since the viscosity of a supercooled liquid at the glass transition temperature is independent of the composition,

$$\eta(T_g(x),x) = \eta(T_g(x_R),x_R). \tag{9}$$

Making use of the Adam–Gibbs relation, we have

$$\frac{T_g(x)}{T_g(x_R)} = \frac{B(x)}{B(x_R)}\frac{S_c(T_g(x_R),x_R)}{S_c(T_g(x),x)}. \tag{10}$$

Assuming the barrier height is a slowly varying function of x,[58,59] $B(x)\approx B(x_R)$ such that

$$\frac{T_g(x)}{T_g(x_R)} = \frac{S_c(T_g(x_R),x_R)}{S_c(T_g(x),x)}. \tag{11}$$

This is a general result. To calculate $T_g(x)$ using Eq. (11), one needs to model $S_c(T,x)$.

The configurational entropy $S_c(T,x)$ of a liquid is related to the degrees of freedom, $f(T,x)=d-n(T,x)$. A system with $f>0$ has f floppy modes per atom. Each floppy mode represents a channel-like pathway in the energy landscape along which a system can explore microstates without increasing its energy significantly. According to Naumis,[60] the configurational entropy associated with the floppy modes is made up of two parts. The major contribution arises from the entropy of the channels themselves. A minor contribution arises from the number of basins having the same value of f (the percolation contribution). According to Naumis,[61] "entropy due to channels in phase space is very likely to be much bigger than the one corresponding to percolation." For this reason, in our treatment we consider only the channel entropy. The channel contribution to the configurational entropy is given by

$$S_c = fNk\ \ln\ \Omega, \tag{12}$$

where Ω is the number of degenerate configurations per floppy mode (proportional to the volume of the phase space explored by a floppy mode). Substituting into Eq. (11), we obtain the composition dependence of T_g,

$$\frac{T_g(x)}{T_g(x_R)} = \frac{f(T_g(x_R),x_R)}{f(T_g(x),x)} = \frac{d-n(T_g(x_R),x_R)}{d-n(T_g(x),x)}. \tag{13}$$

Hence, the glass transition temperature of a composition x can be computed from the composition dependence of the topological constraints.

Equations (4) and (8) also provide an expression for fragility,

$$m(x) \equiv \left.\frac{\partial \log_{10}\ \eta}{\partial(T_g/T)}\right|_{T=T_g(x)} = \frac{B}{T_g S_c(T_g(x),x)}\left(1 + \left.\frac{\partial \ln S_c(T,x)}{\partial \ln T}\right|_{T=T_g(x)}\right). \tag{14}$$

It also follows from Eq. (8) that

$$\log_{10}\left(\frac{\eta_g}{\eta_\infty}\right) = \frac{B}{T_g(x)S_c(T_g(x),x)}. \tag{15}$$

Since $\eta_g=10^{12}$ Pa s and $\eta_\infty\approx 10^{-5}$ Pa s for all compositions,[16] we have

$$m(x) = m_0\left(1 + \left.\frac{\partial \ln S_c(T,x)}{\partial \ln T}\right|_{T=T_g(x)}\right), \tag{16}$$

where $m_0\approx 17$. Substituting Eq. (12) for the configurational entropy, we obtain the desired expression for fragility in terms of f,

$$m(x) = m_0\left(1 + \left.\frac{\partial \ln f(T,x)}{\partial \ln T}\right|_{T=T_g(x)}\right). \tag{17}$$

Using Eq. (17), the fragility of a liquid can be computed based solely on the scaling of the topological degrees of

freedom with temperature. While Eq. (17) can be used, in general, to compute fragility, it is often more convenient to calculate fragility by rewriting the VFT expression of Eq. (1) as[48]

$$m(x) = m_0\left(\frac{T_g(x)}{T_g(x) - T_0(x)}\right). \tag{18}$$

Whereas $T_g(x)$ is an isokomic temperature [see Eq. (3)], $T_0(x)$ is an isentropic temperature,

$$f[T_0(x)] = f[T_0(x_R)] = 0. \tag{19}$$

Thus, with knowledge of $T_g(x)$ and $T_0(x)$, fragility can be computed using Eq. (18).

IV. APPLICATION TO THE BINARY Ge_xSe_{1-x} SYSTEM

In this section, we apply the temperature-dependent constraint model to the binary Ge_xSe_{1-x} system, a covalent system for which much experimental data are available in the literature.[62–73] This system exhibits glass formation continuously from pure Se ($x=0$) to approximately $x=2/5$, which is slightly toward the Ge-rich side of the $x=1/3$ stoichiometric $GeSe_2$ composition. We first review some structural information about the Ge_xSe_{1-x} compositions, starting with $GeSe_2$ ($x=1/3$).

A. Review of structural information

Although some chemical disorder has been reported in $GeSe_2$ glasses,[74,75] it is reasonable to consider that $GeSe_2$ consists of one predominant structural unit—the $GeSe_4$ tetrahedron. The four-coordinated Ge atom sits at the center of the tetrahedron and the selenium atoms occupy the vertices. Each vertex is shared by two tetrahedra such that every selenium atom is coordinated to two germanium atoms. As shown in Fig. 1(a), we refer to such selenium atoms (–Ge–Se–Ge–) as bridging seleniums.

When $x<1/3$ there are more seleniums present than needed to form a network of corner-sharing $GeSe_2$ tetrahedra, as can be readily seen by rewriting the generic composition Ge_xSe_{1-x} as $(GeSe_2)_xSe_{1-3x}$. For $1/5 \le x < 1/3$, the excess selenium atoms are located between neighboring Ge-tetrahedra, forming a bridging selenium pair (–Ge–Se–Se–) as shown in Fig. 1(b). For $x<1/5$, additional selenium atoms are inserted between the tetrahedra, forming chain seleniums (–Se–Se–Se–), indicated in Fig. 1(c).

Compositions in the range of $1/3<x<2/5$ are a mixture of $GeSe_2$ tetrahedra and Ge_2Se_3 structural units, the latter illustrated in Fig. 1(d). The fraction of $GeSe_2$ and Ge_2Se_3 can be computed by introducing a dummy variable y. Balancing the number of germanium atoms,

$$Ge_xSe_{1-x} = (GeSe_2)_{x/3-2y}(Ge_2Se_3)_{x/3+y}, \tag{20}$$

and the number of selenium atoms,

$$2\left(\frac{x}{3} - 2y\right) + 3\left(\frac{x}{3} + y\right) = 1 - x, \tag{21}$$

gives the relation

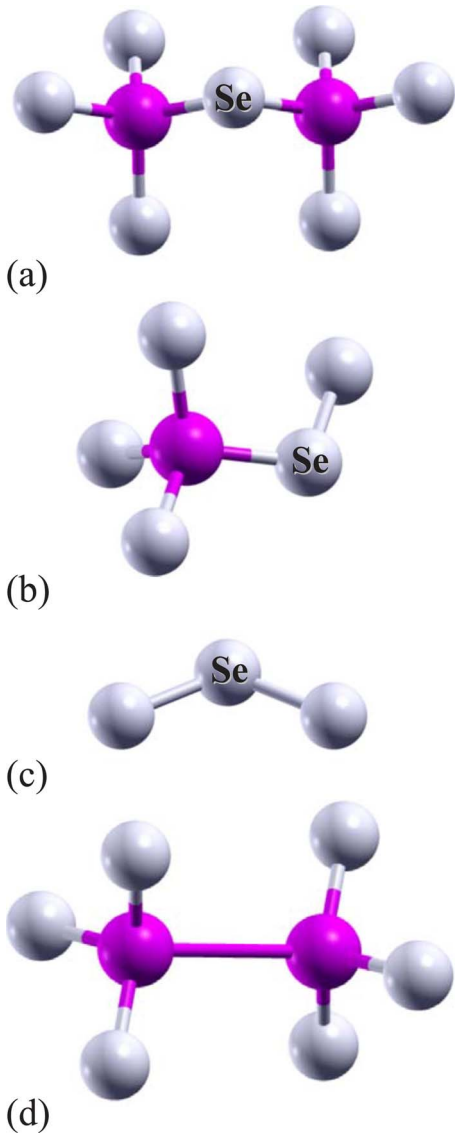

FIG. 1. (Color online) Basic structural units of the Ge_xSe_{1-x} system: (a) bridging selenium connecting two $GeSe_4$ tetrahedra, (b) selenium connecting one $GeSe_4$ tetehedron with one Se–Se rod, (c) chain selenium connecting two Se–Se rods, and (d) the Ge_2Se_3 structural unit.

$$y(x) = \tfrac{8}{3}x - 1. \tag{22}$$

Substituting Eq. (22) into Eq. (20), we obtain

$$Ge_xSe_{1-x} = (GeSe_2)_{2-5x}(Ge_2Se_3)_{3x-1}. \tag{23}$$

B. Calculation of glass transition temperature

In the composition range $0 \le x \le \frac{1}{3}$, the number of constraints per atom is

$$n\left(T, 0 \le x \le \tfrac{1}{3}\right) = x[5q_\alpha(T) + 2q_\beta(T)] + (1-x)[q_\beta(T) + q_\gamma(T)] + q_\delta(T), \tag{24}$$

where $q(T)$ gives the hardness of a particular constraint. The subscripts denote different types of constraints: α represents an Se–Ge–Se angular constraint, β represents a Ge–Se or Se–Se linear bond, γ denotes the angular constraints centered at Se, and δ represents Van der Waals bonding. Hence, the

first term accounts for five angular and two linear constraints at each germanium atom, the second term gives one linear and angular constraint for each selenium atom, and the last term provides for Van der Waals bonding. With the unit step approximation of Eq. (7),

$$n\left(T,0 \le x \le \tfrac{1}{3}\right) = x[5\theta(T_\alpha - T) + 2\theta(T_\beta - T)] + (1-x)[\theta(T_\beta - T) + \theta(T_\gamma - T)] + \theta(T_\delta - T). \tag{25}$$

We assume that the relative strengths of the bonds are such that $T_\delta \le T_\gamma \le T_\beta \le T_\alpha$. The Ge angular constraint (α) is by far the strongest constraint owing to the sp^3 hybridization of the germanium orbitals, which produces rigid tetrahedral bond angles. The linear bond constraints (β) provide the backbone of the glassy network and are frozen in just below the lowest glass transition temperature in our composition space, $T_g(0)$. The Se angular constraint (γ) is known to be quite soft; the elasticity of the Se bond angles is largely responsible for the breakdown of medium-range order in the glassy network.[76] Of course, Van der Waals (δ) forces provide the weakest constraints. With this ordering of bond constraints, the glass transition temperature $T_g(x)$ must fall between T_β and T_α across the full range of x values, i.e.,

$$T_\delta \le T_\gamma \le T_\beta \le T_g\left(0 \le x \le \tfrac{2}{5}\right) \le T_\alpha, \tag{26}$$

in order to satisfy the conditions that $0 < f[T_g(0 \le x \le \frac{2}{5})] < 3$ and $T_g(\frac{2}{5}) > T_g(0)$. [See Eq. (39) and Fig. 3(a) later in this paper.]

With Eq. (26), Eq. (25) simplifies to

$$n\left(T_g(x),0 \le x \le \tfrac{1}{3}\right) = 5x. \tag{27}$$

For a network in three dimensions ($d=3$), the average number of degrees of freedom per atom is

$$f\left(T_g(x),0 \le x \le \tfrac{1}{3}\right) = d - n\left(T_g(x),0 \le x \le \tfrac{1}{3}\right) \tag{28}$$

$$= 3 - 5x. \tag{29}$$

Combining Eqs. (13) and (29), the glass transition temperature can be calculated as

$$\frac{T_g\left(0 \le x \le \frac{1}{3}\right)}{T_g(0)} = \frac{f(T_g(0),0)}{f\left(T_g(x),0 \le x \le \frac{1}{3}\right)} = \frac{3}{3-5x} \tag{30}$$

or

$$T_g\left(0 \le x \le \frac{1}{3}\right) = \frac{1}{1-\frac{5}{3}x} T_g(0), \tag{31}$$

which is exactly the modified Gibbs–DiMarzio equation obtained empirically by Sreeram *et al.*,[77]

$$T_g(\langle r \rangle) = \frac{1}{1 - a(\langle r \rangle - 2)} T_g(0), \tag{32}$$

where $\langle r \rangle$ is the average atomic coordination number. Whereas Sreeram[77] *et al.* obtained a empirically for a variety of three- to five-component chalcogenide systems, here we derive the fitting parameter as $a = 5/6$ for the binary Ge_xSe_{1-x} system (where $\langle r \rangle = 2x+2$). The modified Gibbs–Marzio equation has also been obtained through modeling by Kerner and Micoulaut[78] based on agglomeration of local structures and by Naumis[79] based on the Lindemann criteria and the excess vibrational states due to floppy modes. Kerner and Micoulaut derived the fitting parameter in the limit of low selenium content (i.e., $x \to 0$) as $a = 1/(2 \ln 2) \approx 0.72$, slightly less than our value of $5/6 \approx 0.83$. In Naumis's work, the fitting parameter is obtained using the experimentally measured vibrational density of states in the ternary Ge–As–Se system. Our Eq. (31) shows that in the Ge_xSe_{1-x} system the modified Gibbs–DiMarzio equation is valid only in the composition range of $0 \le x \le 1/3$.

As indicated in Eq. (23), the addition of excess germanium causes formation of Ge_2Se_3 units. For $1/3 \le x \le 2/5$, the number of rigid constraints per atom is given by

$$n\left(T,\tfrac{1}{3} \le x \le \tfrac{2}{5}\right) = (2-5x)[5q_\alpha(T) + 2q_\beta(T)] + (3x-1)[6q_\alpha(T) + 3q_\beta(T) + 6q_\lambda(T)] + (1-x)[q_\beta(T) + q_\gamma(T)] + q_\delta(T), \tag{33}$$

where the new subscript λ refers to additional internal constraints that cause the Ge_2Se_3 unit to become rigid at T_λ. These additional constraints include the Ge–Ge linear constraint, four Ge–Ge–Se bond angle constraints, and a torsion angle constraint. We assume that these constraints are weaker than the Se–Se and Ge–Se linear bonds but stronger than the Se angular constraints: $T_\gamma \le T_\lambda \le T_\beta$. This assumption is clearly justified based on the *ab initio* simulations of Mauro and Varshneya,[75] who showed that the homopolar Ge–Ge bond in these glasses is weaker than both the heteropolar Ge–Se bond and the homopolar Se–Se bond. Moreover, Boolchand *et al.*[72] stated that his "thermal, optical, and nuclear measurements, taken together, show unequivocally that Ge–Ge bonds do *not* form part of the network backbone."

With the unit step approximation of Eq. (7), Eq. (33) becomes

$$n\left(T,\tfrac{1}{3} \le x \le \tfrac{2}{5}\right) = (4-7x)\theta(T_\alpha - T) + (18x-6)\theta(T_\lambda - T) + (1-x)[2\theta(T_\beta - T) + \theta(T_\gamma - T)] + \theta(T_\delta - T). \tag{34}$$

For temperatures near the glass transition, Eq. (26) allows us to simplify as

$$n\left(T_g(x),\tfrac{1}{3} \le x \le \tfrac{2}{5}\right) = 5(2-5x) + 6(3x-1) = 4 - 7x. \tag{35}$$

Hence, the average number of atomic degrees of freedom is given by

$$f\left(T_g(x),\tfrac{1}{3} \le x \le \tfrac{2}{5}\right) = 7x - 1, \tag{36}$$

and the glass transition temperature in the range of $1/3 \le x \le 2/5$ is given by

$$\frac{T_g\left(\frac{1}{3} \le x \le \frac{2}{5}\right)}{T_g(0)} = \frac{f(T_g(0),0)}{f\left(T_g(x),\frac{1}{3} \le x \le \frac{2}{5}\right)} = \frac{3}{7x-1}. \tag{37}$$

We therefore obtain the final result,

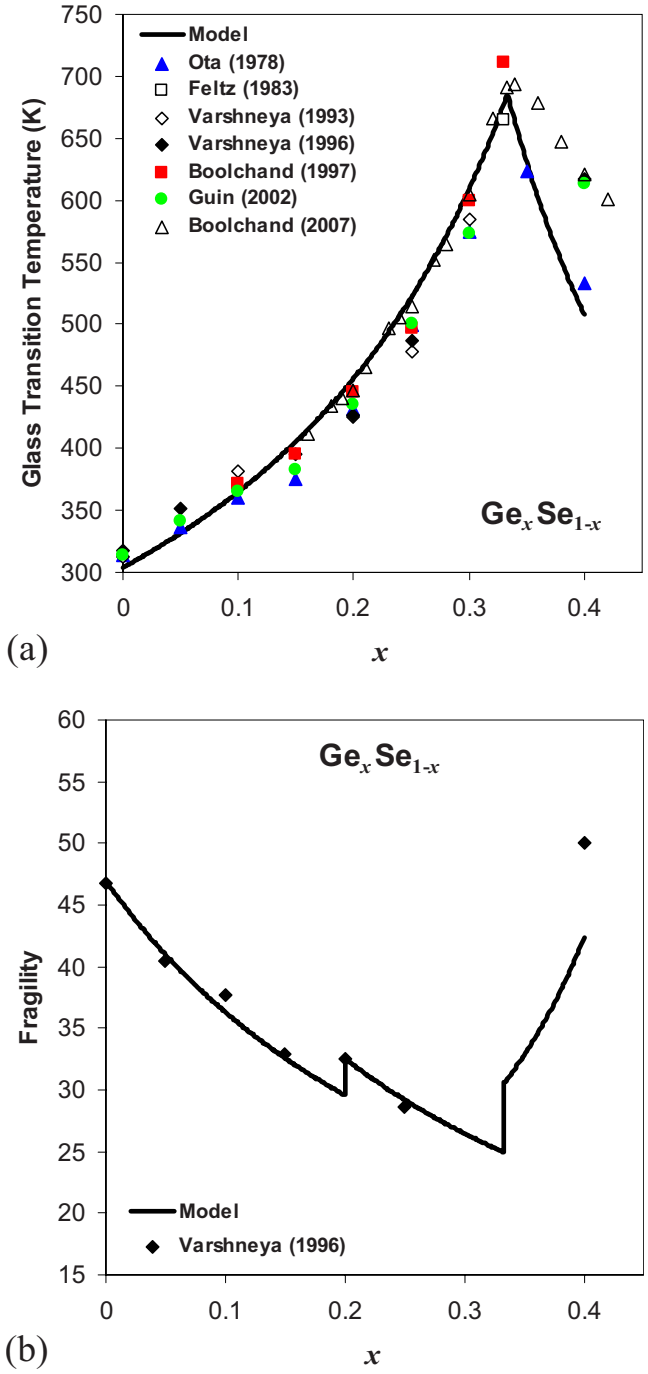

FIG. 2. (Color online) Composition dependence of (a) glass transition temperature and (b) fragility in the Ge_xSe_{1-x} system for $0 \le x \le 2/5$. The solid lines show the predicted values T_g and m using the analytical model of Sec. IV. Results are in good agreement with experimental data (Refs. 62, 63, 66–68, 71, and 72).

$$T_g(x) = \begin{cases} \dfrac{3}{3-5x} T_g(0), & 0 \le x \le \dfrac{1}{3} \\ \dfrac{3}{7x-1} T_g(0), & \dfrac{1}{3} \le x \le \dfrac{2}{5}, \end{cases} \tag{38}$$

which, as shown by the solid line in Fig. 2(a), gives good agreement with experimental measurements without any fitting parameters. The data points in Fig. 2(a) come from several researchers[62,63,66–68,71,72] employing a variety of experimental techniques including viscometry, dilatometry, and calorimetry. While values of T_g can be obtained from any of these methods, use of different techniques effectively involves using different definitions of the glass transition temperature. Hence there is some inherent disagreement among experimental data points, which becomes especially pronounced in the $x > 1/3$ regime. Such Ge-rich glasses are notoriously difficult glass formers; glass quality (including crystallinity and homogeneity) remains a big issue with slowly cooled glasses, and rapid cooling leads to higher values of T_g. The most recent data set is that of Boolchand *et al.*,[72] based on modulated differential scanning calorimetry (DSC). However, our model is built on the viscosity definition of T_g in Eq. (3); our predictions are in better agreement with the data set of Ota *et al.*,[62] based on dilatometry measurements. Since dilatometric T_g is governed directly by flow of the sample, this could provide better agreement with a viscosity-based definition of T_g. In general, DSC-based T_g tends to be higher than viscosity-based T_g (i.e., corresponding to a somewhat lower value of viscosity).[80] Another source of error could be in the model itself, since the structure of the Ge-rich glasses is not well established. While there must be Ge–Ge homopolar bonds, there is also strong evidence for edge sharing of $GeSe_4$ tetrahedra.[72,74,75] Unless these issues are resolved, precise structure based modeling will not be possible. Here we have considered the simplest case of forming Ge_2Se_3 structural units and show that the experimentally observed trend is at least qualitatively predicted by our model.

C. Calculation of T_0 and fragility

Using Eq. (18) we can compute the composition dependence of fragility, $m(x)$, from a knowledge of $T_g(x)$ and $T_0(x)$. As discussed previously, $T_0(x)$ is the temperature at which the degrees of freedom vanish: $f[T_0(x),x]=0$. From Eqs. (25) and (34), the temperature and composition dependence of f is given by

$$f(T,x) = \begin{cases} \begin{cases} 3, & T > T_\alpha \\ 3-5x, & T_\beta < T < T_\alpha \\ 2-6x, & T_\gamma < T < T_\beta, \\ 1-5x, & T_\delta < T < T_\gamma \\ -5x, & T < T_\delta \end{cases} & 0 \le x \le \frac{1}{3} \\ \begin{cases} 3, & T > T_\alpha \\ 7x-1, & T_\beta < T < T_\alpha \\ 9x-3, & T_\lambda < T < T_\beta, \\ 3-9x, & T_\gamma < T < T_\lambda \\ 2-8x, & T_\delta < T < T_\gamma \\ 1-8x, & T < T_\delta \end{cases} & \frac{1}{3} \le x \le \frac{2}{5}, \end{cases} \tag{39}$$

which is plotted in Fig. 3(a). This figure shows three distinct values of T_0,

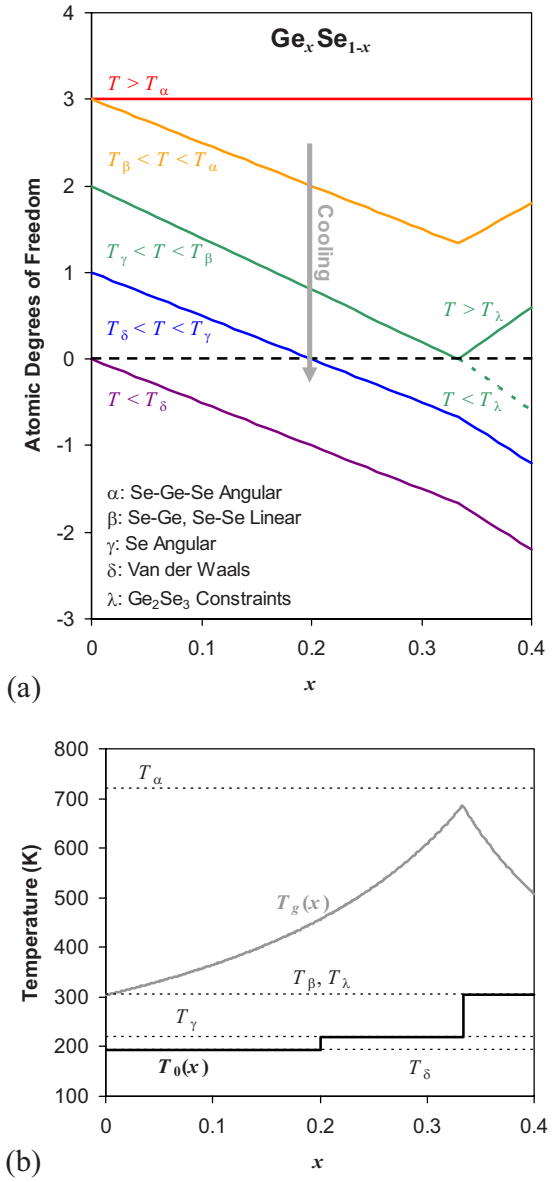

FIG. 3. (Color online) (a) The temperature and composition dependence of the average number of atomic degrees of freedom in the Ge_xSe_{1-x} system, including linear bonds, angular constraints, and Van der Waals bonding. (b) Plot of the critical temperatures: $T_\alpha > 700$ K, $T_\beta = T_\lambda = T_g(0) = 304$ K, $T_\gamma = 218$ K, and $T_\delta = 194$ K. $T_0(x)$ corresponds to the highest temperature where all degrees of freedom have vanished. The glass transition temperature $T_g(x)$ falls between T_β and T_α for all x.

$$T_0(x) = \begin{cases} T_\delta, & 0 \le x < \frac{1}{5} \\ T_\gamma, & \frac{1}{5} \le x < \frac{1}{3} \\ T_\lambda, & \frac{1}{3} \le x \le \frac{2}{5}, \end{cases} \tag{40}$$

indicated also in Fig. 3(b). Here we optimize $T_\delta = 194$ K and $T_\gamma = 218$ K to the fragility data of Senapati and Varshneya,[67] and we maximize the final $T_\lambda = 304$ K. [All three temperatures must fall below $T_g(0)$, or else the assumption of Eq. (26) is violated.] As shown in Fig. 2(b), we demonstrate excellent agreement with experiment except for underpredicting the final data point at $x = 2/5$. There is a small step in $m(x)$ at $x = 1/5$ owing to the change in T_0 from T_δ (i.e., governed by Van der Waals constraints) to T_γ (i.e., governed by Se angular constraints). This discontinuity results from the unit step approximation of Eq. (7) and will be smoothed out for a real system. There is a larger discontinuity at $x = 1/3$ as T_0 becomes dominated by the internal constraints of the Ge_2Se_3 unit.

V. CONCLUSIONS

We have presented a general topological modeling approach accounting for the temperature-dependent nature of the network constraints. Our approach is a generalization of the previous work of Phillips and Thorpe[33–38] and of Gupta and Cooper[39–43] and allows for calculation of the composition dependence of glass transition temperature and fragility. We have applied the new approach to the binary Ge_xSe_{1-x} system and shown excellent agreement of $T_g(x)$ and $m(x)$ with experimental data.

The main advantage of our approach lies in its simplicity and the ability to obtain concise analytical expressions for the scaling of glass transition temperature and fragility with composition. It is currently not possible to compute such properties from traditional atomistic simulation techniques such as molecular dynamics, as these techniques cannot access the long time scales necessary to compute viscosity near the glass transition.

However, unlike molecular dynamics our topological approach assumes *a priori* knowledge of the basic structural units of the glass-forming liquid, as well as the relative strengths of the different constraints. Atomistic or quantum-level simulations could be used to provide this input into the topological model. In this manner, the topological model can be treated as one level of a broader multiscale modeling approach, where structural and bond strength information from numerical simulations are fed as input into the topological model, which is then used to predict the scaling of macroscopic properties. Based on the previous work of Mauro and Varshneya,[73,75,81,82] we believe that Metropolis Monte Carlo simulations will be particularly useful in this regard, as they can provide accurate structural information more efficiently compared to classical molecular dynamics.[9]

One drawback of the current approach is the assumption of mean-field theory in describing the rigidity of the network. While mean-field theory is known to provide a good approximation of rigidity percolation,[33–38] corrections due to local stress effects are crucial for understanding the so-called intermediate phase behavior.[83,84] Also, our current approach ignores the presence of defects such as miscoordinated atoms or edge-sharing tetrahedra, features that are known to occur in chalcogenide systems;[74,75] however, it should be possible to extend our treatment to include the presence of such defects.

ACKNOWLEDGMENTS

We take great pleasure in acknowledging valuable discussions with Roger J. Loucks and Arun K. Varshneya of Alfred University, Bruce Patton of Ohio State University, and Douglas C. Allan, Marcel Potuzak, Amy L. Rovelstad, and Kamal Soni of Corning Inc.. We also greatly appreciate helpful comments and encouragement from James C. Phil-

lips (Rutgers University), Punit Boolchand and Ping Chen (University of Cincinnati), and Gerardo G. Naumis (Universidad Nacional Autónoma de México).

[1] A. K. Varshneya, *Fundamentals of Inorganic Glasses*, 2nd ed. (Society of Glass Technology, Sheffield, 2006).
[2] J. Zarzycki, *Glasses and the Vitreous State* (Cambridge University Press, Cambridge, 1990).
[3] D. R. Uhlmann and N. J. Kreidl, *Glass: Science and Technology* (Academic, New York, 1983).
[4] P. B. Macedo and A. Napolitano, J. Res. Natl. Bur. Stand., Sect. A **71**, 231 (1967).
[5] A. Napolitano, J. H. Simmons, D. H. Blackburn, and R. E. Chidester, J. Res. Natl. Bur. Stand., Sect. A **78**, 323 (1974).
[6] C. A. Angell and D. L. Smith, J. Phys. Chem. **86**, 3845 (1982).
[7] D. Alfe and M. J. Gillian, Phys. Rev. Lett. **81**, 5161 (1998).
[8] C. Hoheisel, Phys. Rep. **245**, 111 (1994).
[9] L. Wondraczek and J. C. Mauro, J. Eur. Ceram. Soc. DOI:10.1016/j.jeurceramsoc.2008.08.006.
[10] G. Adam and J. H. Gibbs, J. Chem. Phys. **43**, 139 (1965).
[11] G. W. Scherer, J. Am. Ceram. Soc. **67**, 709 (1984).
[12] Y. Bottinga and P. Richet, Chem. Geol. **128**, 129 (1996).
[13] M. D. Ediger, C. A. Angell, and S. R. Nagel, J. Phys. Chem. **100**, 13200 (1996).
[14] R. Richert and C. A. Angell, J. Chem. Phys. **108**, 9016 (1998).
[15] J.-P. Bouchaud and G. Biroli, J. Chem. Phys. **121**, 7347 (2004).
[16] C. A. Angell, J. Non-Cryst. Solids **73**, 1 (1985).
[17] C. A. Angell, J. Non-Cryst. Solids **102**, 205 (1988).
[18] C. A. Angell, J. Non-Cryst. Solids **131–133**, 13 (1991).
[19] C. A. Angell, K. L. Ngai, G. B. McKenna, P. F. McMillan, and S. W. Martin, J. Appl. Phys. **88**, 3113 (2000).
[20] R. Böhmer and C. A. Angell, Phys. Rev. B **45**, 10091 (1992).
[21] A. P. Sokolov, E. Rössler, A. Kisliuk, and D. Quitmann, Phys. Rev. Lett. **71**, 2062 (1993).
[22] S. Sastry, Nature (London) **409**, 164 (2001).
[23] L. Larini, A. Ottochian, C. de Michele, and D. Leporini, Nat. Phys. **4**, 42 (2008).
[24] L.-M. Martinez and C. A. Angell, Nature (London) **410**, 663 (2001).
[25] C. A. Angell, Chem. Rev. (Washington, D.C.) **102**, 2627 (2002).
[26] T. Scopigno, G. Ruocco, F. Sette, and G. Monaco, Science **302**, 849 (2003).
[27] V. N. Novikov and A. P. Sokolov, Nature (London) **431**, 961 (2004).
[28] S. N. Yannopoulos and G. P. Johari, Nature (London) **442**, E7 (2006).
[29] J. C. Dyre, Rev. Mod. Phys. **78**, 953 (2006).
[30] K. Niss, C. Dalle-Ferrier, G. Tarjus, and C. Alba-Simionesco, J. Phys.: Condens. Matter **19**, 076102 (2007).
[31] L. Hornbøll and Y. Yue, J. Non-Cryst. Solids **354**, 350 (2008).
[32] J. C. Mauro and R. J. Loucks, Phys. Rev. E **78**, 021502 (2008).
[33] J. C. Phillips, J. Non-Cryst. Solids **34**, 153 (1979).
[34] J. C. Phillips and M. F. Thorpe, Solid State Commun. **53**, 699 (1985).
[35] M. F. Thorpe, J. Non-Cryst. Solids **57**, 355 (1983).
[36] H. He and M. F. Thorpe, Phys. Rev. Lett. **54**, 2107 (1985).
[37] Y. Cai and M. F. Thorpe, Phys. Rev. B **40**, 10535 (1989).
[38] M. F. Thorpe, J. Non-Cryst. Solids **182**, 135 (1995).
[39] A. R. Cooper, Phys. Chem. Glasses **19**, 60 (1978).
[40] P. K. Gupta and A. R. Cooper, J. Non-Cryst. Solids **123**, 14 (1990).
[41] P. K. Gupta, J. Am. Ceram. Soc. **76**, 1088 (1993).
[42] P. K. Gupta, in *Rigidity Theory and Applications*, edited by M. F. Thorpe and P. M. Duxbury (Kluwer, New York, 1999), p. 173.
[43] P. K. Gupta and D. B. Miracle, Acta Mater. **55**, 4507 (2007).
[44] M. Goldstein, J. Chem. Phys. **51**, 3728 (1969).
[45] F. H. Stillinger, J. Phys. Chem. B **102**, 2807 (1998).
[46] T. F. Middleton and D. J. Wales, J. Chem. Phys. **118**, 4583 (2003).
[47] J. C. Mauro, R. J. Loucks, and J. Balakrishnan, J. Phys. Chem. B **110**, 5005 (2006).
[48] J. C. Mauro and R. J. Loucks, Phys. Rev. B **76**, 174202 (2007).
[49] J. C. Mauro, R. J. Loucks, A. K. Varshneya, and P. K. Gupta, Sci. Model. Simul. **15**(1), 241 (2008).
[50] F. H. Stillinger and T. A. Weber, Phys. Rev. A **25**, 978 (1982).
[51] F. H. Stillinger and T. A. Weber, Phys. Rev. A **28**, 2408 (1983).
[52] F. H. Stillinger, J. Chem. Phys. **88**, 7818 (1988).
[53] P. G. Debenedetti, F. H. Stillinger, T. M. Truskett, and C. J. Roberts, J. Phys. Chem. B **103**, 7390 (1999).
[54] P. G. Debenedetti and F. H. Stillinger, Nature (London) **410**, 259 (2001).
[55] F. H. Stillinger and P. G. Debenedetti, J. Chem. Phys. **116**, 3353 (2002).
[56] P. K. Gupta and J. C. Mauro, J. Chem. Phys. **126**, 224504 (2007).
[57] J. H. Gibbs and E. A. DiMarzio, J. Chem. Phys. **28**, 373 (1958).
[58] M. J. Toplis, Am. Mineral. **83**, 480 (1998).
[59] M. J. Toplis, Chem. Geol. **174**, 321 (2001).
[60] G. G. Naumis, Phys. Rev. E **71**, 026114 (2005).
[61] G. G. Naumis, J. Non-Cryst. Solids **352**, 4865 (2006).
[62] R. Ota, T. Yamate, N. Soga, and M. Kunugi, J. Non-Cryst. Solids **29**, 67 (1978).
[63] A. Feltz, H. Aust, and A. Blayer, J. Non-Cryst. Solids **55**, 179 (1983).
[64] S. Susman, K. J. Volin, D. G. Montague, and D. L. Price, J. Non-Cryst. Solids **125**, 168 (1990).
[65] N. Afify, Phys. Rev. B **48**, 16304 (1993).
[66] A. K. Varshneya, A. N. Sreeram, and D. R. Swiler, Phys. Chem. Glasses **34**, 179 (1993).
[67] U. Senapati and A. K. Varshneya, J. Non-Cryst. Solids **197**, 210 (1996).
[68] X. Feng, W. J. Bresser, and P. Boolchand, Phys. Rev. Lett. **78**, 4422 (1997). (We thank these authors for providing us with actual numerical values of data shown in their Fig. 1.)
[69] N. R. Rao, P. S. R. Krishna, S. Basu, B. A. Dasannacharya, K. S. Sangunni, and E. S. R. Gopal, J. Non-Cryst. Solids **240**, 221 (1998).
[70] P. Boolchand, X. Feng, and W. J. Bresser, J. Non-Cryst. Solids **293–295**, 348 (2001).
[71] J.-P. Guin, T. Rouxel, V. Keryvin, J.-C. Sanglebœuf, I. Serre, and J. Lucas, J. Non-Cryst. Solids **298**, 260 (2002).
[72] P. Boolchand, P. Chen, M. Jin, B. Goodman, and W. J. Bresser, Physica B **389**, 18 (2007) (We thank the authors for providing us with the raw data points, including additional data not published in the current paper.).
[73] J. C. Mauro and A. K. Varshneya, J. Am. Ceram. Soc. **90**, 192 (2007).
[74] I. Petri, P. S. Salmon, and H. E. Fischer, Phys. Rev. Lett. **84**, 2413 (2000).
[75] J. C. Mauro and A. K. Varshneya, J. Am. Ceram. Soc. **89**, 2323 (2006).
[76] R. Kerner, Glass Phys. Chem. **26**, 313 (2000).
[77] A. N. Sreeram, D. R. Swiler, and A. K. Varshneya, J. Non-Cryst. Solids **127**, 287 (1991).
[78] R. Kerner and M. Micoulaut, J. Non-Cryst. Solids **210**, 298 (1997).
[79] G. G. Naumis, Phys. Rev. B **73**, 172202 (2006).
[80] C. T. Moynihan, J. Am. Ceram. Soc. **76**, 1081 (1993).
[81] J. C. Mauro and A. K. Varshneya, Phys. Rev. B **71**, 214105 (2005).
[82] J. C. Mauro and A. K. Varshneya, Phys. Rev. B **72**, 024212 (2005).
[83] Y. Wang, P. Boolchand, and M. Micoulaut, Europhys. Lett. **52**, 633 (2000).
[84] M. Micoulaut and J. C. Phillips, Phys. Rev. B **67**, 104204 (2003).